On the mechanism of long-range alignment order of fibroblasts

Xuefei Li
Center for Theoretical Biological Physics, Rice University, 6500 Main Street, Houston Texas 77030, USA

Rajesh Balagam
*Department of Bioengineering, Rice University, 6500 Main Street, Houston Texas 77030, USA**

Ting-Fang He and Peter P. Lee
Immuno-Oncology, City of Hope Comprehensive Cancer Center, 1500 East Duarte Road, Duarte, CA 91010, USA

Oleg A. Igoshin† and Herbert Levine‡
Department of Bioengineering, Rice University, 6500 Main Street, Houston Texas 77030, USA and Center for Theoretical Biological Physics, Rice University, 6500 Main Street, Houston Texas 77030, USA*

(Dated: March 23, 2017)

Long-range alignment ordering of fibroblasts have been observed in the vicinity of cancerous tumors and can be recapitulated with *in vitro* experiments. However, the mechanisms driving their ordering are not understood. Here we show that local collision-driven nematic alignment interactions among fibroblasts are insufficient to explain observed long-range alignment. One possibility is that there exists another orientation field co-evolving with the cells and reinforcing their alignment. We propose this field reflects the mechanical cross-talk between the fibroblasts and the underlying fibrous material on which they move. We demonstrate that this new long-range interaction can give rise to high nematic order and to the observed patterning of the cancer microenvironment.

Usage:

PACS numbers:

Structure:

Fibroblasts are spindle shaped cells that are highly motile and are involved in many critical biological processes such as wound healing. Recently, their major role in shaping the local micro-environment around a growing tumor was show in numerous studies [1–3]. As a result, fibroblasts can affect the ability of cancer cells to metastasize [4–6] and conversely the ability of the immune system to find and attack those cells [7].

Curiously, imaging of tumor micro-environments often indicates long-range ordering of fibroblasts. This order often takes the form of circumferential alignment of the cells in a region surrounding the cancer cells - see Fig. 1(a). Notably, a similar ordering can be observed for underlying collagen fibers (Fig. 1(b)). Collagen fibers are the main structural component in the extracellular space of various normal connective tissues and play a significant role in cancer progression [11].

Long-range ordering can also be recapitulated in two dimensional cell culture experiments. In particular, Duclos et al. [10] generated quantitative measurements of cluster orientation as fibroblasts move, collide, and proliferate (grow and divide) on cover slips in 2D. They measured the population averaged nematic order parameter $Q = \sqrt{< \cos 2\theta_i >^2 + < \sin 2\theta_i >^2}$, which decreases from 1 for perfectly aligned to 0 for randomly oriented cell population. It was observed that the nematic order gradually increases with cell density as it increases due to cell growth. After roughly 80 hrs, cell motions become significantly limited due to jamming. Consequently, nematic order will freeze at a fixed value. Very interestingly, for the particular case of a channel-like geometry, as long as the channel width is smaller than the characteristic orientation-correlation length, perfect nematic order can be robustly observed.

An isolated fibroblast moves back and forth on cover slips for over 60 hours without significant change of the direction of its major axis [10]. Typically, those fibroblasts are in a spindle shape with an aspect ratio from 2 to 5. Apart from steric constraints, fibroblasts barely interact with each other [10].

Steric interactions between fibroblast can lead to their locally alignment. It is therefore interesting to determine if the experimental results described above can in fact be explained by treating fibroblasts as apolar active particles with hard collision interactions (active nematics). In this work we show that the answer is no. We therefore propose one possible new mechanism, which couples cells through their mutual effect on their mechanical environment. This coupling can recapitulate the observed ordering and explain the observed connection between fibroblast and collagen orientation patterns Fig. 1(b). Furthermore, our model offers specific predictions testable with new cell culture experiments.

* The first two authors contributed equally
† igoshin@rice.edu
‡ herbert.levine@rice.edu

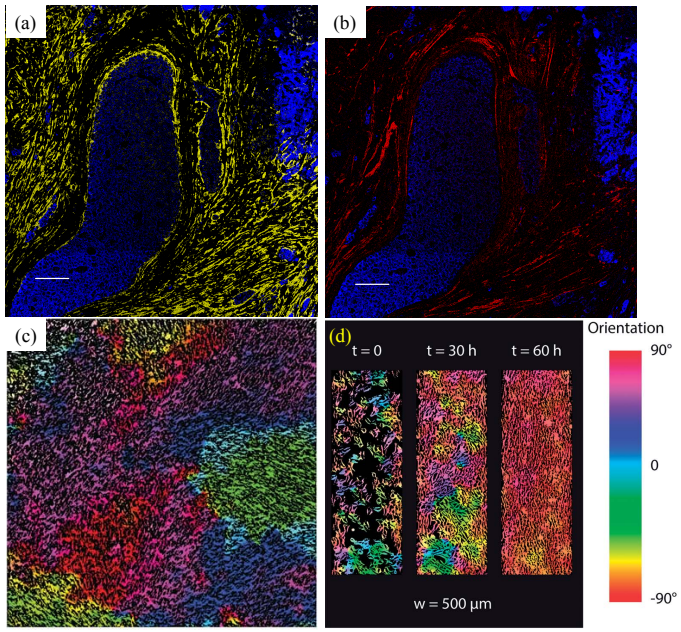

FIG. 1. (a) A breast cancer specimen from a patient. One particular protein–alpha smooth muscle actin, which is expressed by cancer associated fibroblasts [8] in cancerous tissue, is labeled in yellow. Cancer cells are labeled in blue. These fibroblasts are found mostly in the space between cancer-cell clusters and orient azimuthally around the clusters. Scale Bar 100 μm (white, left corner). (b) The same field of view as in (a). Collagen fibers captured by a Second Harmonic Generation microscope [9] are labeled in red. They surround the breast cancer cells (blue) and are parallel to the boundary of the cancer-cell clusters. Scale Bar 100 μm (while, left corner). (c)(d) Figures adapted from Ref. [10]. (c) Color-Coded orientation of fibroblasts on a 2D plate. Field of view is 1.5mm×1.5mm. (d) Evolution of perfect nematic alignment of fibroblasts in a 2D channel. Width of channel is 0.5mm.

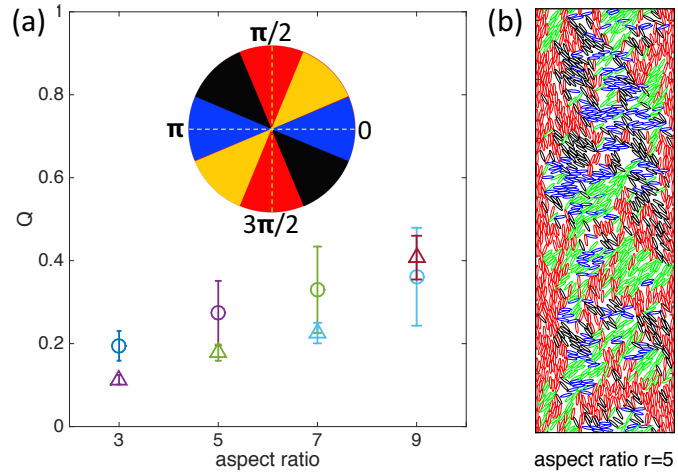

FIG. 2. In those simulations, channels are set as $24rb$ across horizontal axis and $360b$ across vertical axis, therefore there can be up to 2000 particles in the simulation. In all simulations, $b = 1$. Periodic boundary condition is applied along the vertical axis. Two hard walls are implemented on the left and right. If possible, one particle is introduced into the system every simulation time step and one simulation time step corresponds to 0.05 hour in real time. This mimics the cell density increase observed in experiments. (a) Nematic order in a channel. Values of nematic order parameter are shown as circles for elliptic particles described in the main text or as triangles for capsules with a more realistic physical model described in SI. For simulations of elliptic particles, aspect ratio $r = 3, 5, 7, 9$, reversal probability $p = 0.1$, and self-propelled velocity $v = 0.1, 0.1667, 0.2333, 0.3$ for different r. Particle number gradually increases from 300 (packing fraction 0.11) to about 1600 (packing fraction 0.58). The number of simulation steps is 2000, which corresponds to around 100 hours in real time. For simulations of capsules, detailed procedures and parameters are described in SI. (b) A snapshot of the simulation at step 2000 for ellipses with aspect ratio 5.

We start with a simple active nematics model representing fibroblasts as hard elliptic particles with the major radius a, the minor radius b and the aspect ratio $r = a/b$. Particles move back and forth and interact simply via collisions. Each elliptic particle moves along its major axis with a constant velocity v and a reversal probability p. A particle also randomly moves along its minor axis with a small amplitude. These mimic the motion of an isolated fibroblasts observed by Duclos et al. [10]. A more detailed description of the translational motion is presented in the supplementary information (SI).

At each time step, we propose a new position of all elliptic particles along their major and minor axes. If particles with new positions overlap with boundaries or their neighbors, a particle is made to retreat and a new orientation will be proposed to avoid further overlaps. If not, the new positions will be updated. We perform particle reorientations within one simulation time step in a sequential fashion for all particles. And the sequence of particles is randomly permuted after each simulation time step. To mimic the fibroblast proliferation observed in experiments, new particles are being added in front of randomly selected particles and with the same orientation as the selected particle. More detailed aspects of our procedures, such as how a particle aligns with boundaries and how new orientations are proposed after particle collisions, are described in the supplementary information.

With these collision-like interactions, our simulations (Fig. 2) did not reproduce the perfect nematic order among particles for channels as wide as 60 particles across. In contrast, experiments in [10] showed the nearly-perfect alignment of fibroblasts to the channel boundaries up-to a channel width of $500\mu m$, where the width of a fibroblast is around $5\mu m$. In our simulations, while particles right next to channel boundaries align parallel to boundaries, this alignment disappears for cells in the channel center, Fig. 2(b). Altering the simulation to higher aspect ratio (up to 9) does not result in a perfect nematic ordering, Fig. 2(a).

Our results are not totally surprising in light of some previous studies. For point-like particles with nematic

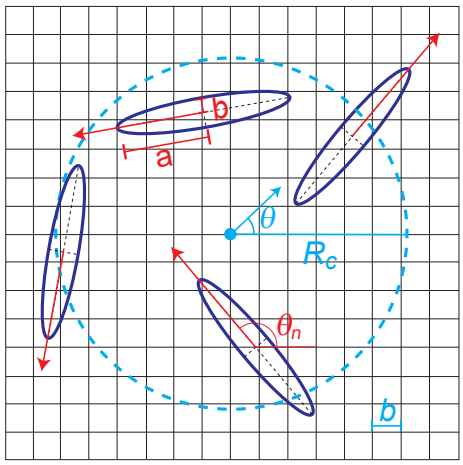

FIG. 3. Illustration of our proposed mechanism. A cyan dot emphasizes a specific grid point on which we consider the orientation field. Elliptic particles falling within the dashed circle (radius, R_c) will affect the orientation field at that grid point. The cyan arrow at the center of the circle indicates the current direction of that orientation field. Each particle's current orientation is denoted by a red arrow from its center and it will bias the orientation field towards its direction; this is described quantitatively by Eq. (1).

interactions described by a Vicsek type model [12], there can be high nematic order in a low rotational noise regime. However, the results are different for hard eliptic particles. Shi and Ma [13] performed kinetic Monte-Carlo simulations of such particles moving back and forth and colliding on the 2D surface, which mimics experiments carried out by Narayan et al. [14]. The results indicate that, unlike particles performing Brownian motions, nematic order for active nematics gradually decreases with increase in particle density. Direction reversal of self-propelled particles can also play a key role, as it can disrupt nematic order or cell-clustering [15, 16]. There also have been recent analytical work [17] showing that highly ordered state can be unstable in active nematics.[18]

We have investigated a wide variety of modifications of our basic model, without any significant change in the results (see SI). We therefore conclude that a new mechanism is needed. Motivated by [15], we propose a novel mechanism in which there exists an orientation field coupled to nearby particles and that this field can in turn affect the orientation of those particles. For fibroblasts, this idea is supported by the fact that cells secrete materials for extracellular matrix (ECM) such as collagen [19, 20]. Furthermore, as fibroblasts move, they contract and align ECM fibers depending on their direction of motion [21, 22]. Recent experimental results also show that a fiber network under strain over a threshold time can change its structural and properties in a non-reversible fashion [23]. As a result, the fiber network at some point can "remember" the average orientation of the particles that have previously traversed close to that location. We hypothesize that co-evolution of ECM network and fibroblasts drives the emergence of the patterns in cancer tissue specimens and the high nematic order in culture.

Rather than formulate an extremely detailed mechanical model of ECM-fibroblast co-orientation, we have opted for a simple proof-of-principle phenomenological approach as illustrated in Fig. 3. The orientation field θ of each grid point will be affected by the orientations of particles θ_n within a radius of R_c surrounding that grid point in a time dependent manner. Specifically, the orientation field of each grid point will be updated according to Eq. (1).

$$\frac{d\theta}{dt} = \alpha \frac{1}{M} \sum_{n=1}^{M} \frac{1}{2} \sin\left[2\left(\theta_n - \theta\right)\right], \tag{1}$$

where M is the number of particles within a radius R_c of each grid point. For small α (field update strength), the orientation field slowly responds to nearby fibroblasts and has a long memory of previous motion in its vicinity. With an updated orientation field, a new orientation of each particle is proposed to equal θ of its closest grid point. Translational motion of the particle is then proposed according to this new orientation. The subsequent steps are then the same as in the simple active nematic model described before.

With the above mechanism, it is now possible to attain high order. Particularly, for the channel-like confinement setup, nearly-perfect nematic order can be realized for width of channel over 60 particles across. In this case, cells close to the hard walls move around and orient themselves to align with the wall. Then this orientation propagates into the channel center. These features are quite similar to those reported by Duclos et al. [10]. The results are shown in Fig. 4(a) and (b) and quantified in Fig. 4(c) and (d). We should note that for the simulations in the channel case, even with long-range interactions, there are still 2 cases out of 8 simulations which stay at a high order but not nearly-perfect alignment. In those cases, defects developed close to the boundary and did not resolve before the particle density increased to a level that the jamming effect kicked in.

We now add obstacles to our simulation, mimicking the effect of the cancer-cell clusters around which the fibroblasts move and proliferate. We found that if new elliptic particles are introduced into the simulation box with the same probability everywhere, i.e. the "proliferation rate" of a particle does not depend on its location, it is easy to find clusters of particles pointing towards an obstacle instead of circumferentially aligning around the boundary of an obstacle. Since it takes some time before particles align to the boundary of an obstacle and re-organize the orientation field around an obstacle, jamming effects due to high particle density can hinder the circumferential alignment. Therefore, it is important to ensure that particles around an obstacle do not jam before they align with the boundary.

To avoid this possible jamming and help propose an explanation for the circumferential patterns seen e.g. in

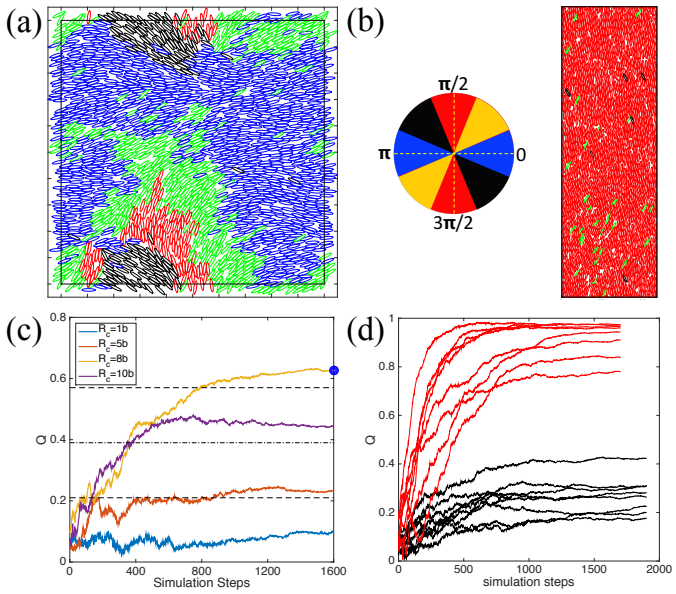

FIG. 4. Numerical simulations generating long-range alignment order. The number of particles gradually increases from 300 to over 1500 in the simulations, i.e., the packing fraction increases from 0.12 up-to 0.58. The aspect ratio of particles in these examples is chosen as 5. α is chosen as 0.1 in those simulations. (a) A snapshot of the particle configuration of one simulation at step 1600 for periodic boundary condition, which corresponds to nematic order of the blue dot in (c). (b) A snapshot of the particle configuration of one simulation at step 1000 for a channel-like structure. (c) These simulations are carried out in a box with periodic boundary condition. Different solid lines represent evolution of the nematic order by varying the range of interaction R_c in Fig. 3. Dash-dotted line is the sample average given in the paper by Duclos et al. [10] and dashed lines are the standard deviations. It is interesting to notice that increasing R_c does not always give rise to a higher order. (d) Different realizations of our stochastic simulation carried out in a channel-like structure. Red lines represent the evolution of nematic order with long-range interactions applied ($R_c = 15b$). For comparison, black lines are different realizations of the system with only collision interactions.

Fig. 1, we introduce one other feature, namely that new elliptic particles be introduced with a higher probability in a range close to the obstacles. Therefore, particles can get out of a local jamming through moving away from an obstacle. This assumption is based again on the observations of [10], that fibroblasts closer to boundaries proliferate faster. This may also be a feature of the cancer micro-environment where fibroblasts may be stimulated by growth factors released by the tumor. With this new ingredient applied in the simulation, we can now generate the pattern in which the ellipses as well as orientation field align azimuthally around obstacles. These results are shown in Fig. 5(a) and (b), and the resulting patterns closely resemble the experimentally observed ones shown in Fig. 1.

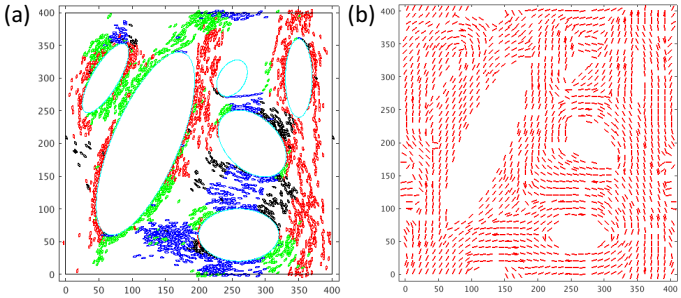

FIG. 5. Numerical simulations with proposed mechanism applied. Hard elliptic obstacles were assigned beforehand. 400 particles were first randomly assigned. New particles are added only within a small range close to large obstacles. Color-coding of elliptic particles are the same as that in Fig. 2(b). Distribution of fibroblasts is shown in (a). Orientation field is shown in (b). Qualitatively, the simulation results are comparable to experimental result shown in Fig. 1.

In conclusion, in this paper we propose a new mechanism that explains long-range ordering patterns of fibroblasts: azimuthal alignment around cancer-cell clusters (Fig. 5(a)) and the nearly-perfect nematic order in 2D channel cultures (Fig. 4(b)). Specifically, we propose that fibroblasts may align with each other through nonlocal interactions arising from their modification of an underlying ECM network. We demonstrated that such a long-range interaction is necessary to even qualitatively reproduce experimental observations (e.g., Fig. 4(c)(d)). The proposed mechanism can be tested in future experiments that monitor cancer tissues with live imaging to show the temporal co-evolution of fibroblasts and ECM network or directly image deposited biopolymers in the culture experiments. The model would predict the co-evolution in the orientation of fibroblasts and corresponding ECM networks. On the other hand, if the accumulation of ECM materials or the interaction between fibroblasts and underlying ECM networks is significantly disrupted (e.g. by mutation), the model would predict a diminished long-range alignment order of fibroblasts.

This work was supported by the National Science Foundation Center for Theoretical Biological Physics (NSF PHY-1427654), and NSF DMS-1361411, Stand Up to Cancer, and The V Foundation. O.A.I. and R.B. are supported by NSF MCB-1411780. H.L. is also a Cancer Prevention and Research Institute of Texas (CPRIT) Scholar in Cancer Research of the State of Texas at Rice University. We thank the research associates Roger Wang and Anthony Rosario from P.L. group at the City of Hope for antibody staining and manuscript editing; the Ultima Intra-Vital system is supported by the Light Microscopy Core and Shared Resources at the City of Hope (Duarte, CA). We also thank Dr. Brian Armstrong (director of Light Microscopy Core at City of Hope) for editing part of the manuscript.

[1] N. Bhowmick, E. Neilson, and H. Moses, Nature **432**, 332 (2004).

[2] R. Kalluri and M. Zeisberg, Nat. Rev. Cancer **6**, 392 (2006).

[3] K. K. Pietras and A. Östman, Exp. Cell. Res. **316**, 1324 (2010).

[4] P. Provenzano, K. Eliceiri, J. Campbell, D. Inman, J. White, and P. Keely, BMC medicine **4**, 1 (2006).

[5] R. Hwang, T. Moore, T. Arumugam, V. Ramachandran, K. Amos, A. Rivera, B. Ji, D. Evans, and C. Logsdon, Cancer Res. **68**, 918 (2008).

[6] Y. Zhang, H. Tang, J. Cai, T. Zhang, J. Guo, D. Feng, and Z. Wang, Cancer Lett. **303**, 47 (2011).

[7] E. Peranzoni, A. Rivas-Caicedo, H. Bougherara, H. Salmon, and E. Donnadieu, Cell. Mol. Life Sci. **70**, 4431 (2013).

[8] M. Augsten, Front. Oncol. **4**, 62 (2014).

[9] G. Cox and E. Kable, Methods Mol. Biol. **319**, 15 (2006).

[10] G. Duclos, S. Garcia, H. G. Yevick, and P. Silberzan, Soft matter **10**, 2346 (2014).

[11] M. W. Conklin, J. C. Eickhoff, K. M. Riching, C. A. Pehlke, K. W. Eliceiri, P. P. Provenzano, A. Friedl, and P. J. Keely, Am. J. Pathol. **178**, 1221 (2011).

[12] H. Chaté, F. Ginelli, and R. Montagne, Phys. Rev. Lett **96**, 180602 (2006).

[13] S. Shi and Y. Ma, Nat. Commun. **4** (2013).

[14] V. Narayan, S. Ramaswamy, and N. Menon, Science **317**, 105 (2007).

[15] R. Balagam and O. A. Igoshin, PLoS Comput. Biol. **11**, e1004474 (2015).

[16] R. Großmann, F. Peruani, and M. Bär, Phys. Rev. E **94**, 050602(R) (2016).

[17] X. Shi, H. Chaté, and Y. Ma, New J. Phys **16**, 035003 (2014).

[18] Very recently, via private communications we became aware that a team led by Bates and Sahai have developed computational models of nematic ordering considering volume exclusion effects explicitly.

[19] F. Grinnell, H. Fukamizu, P. Pawelek, and S. Nakagawa, Exp. Cell. Res. **181**, 483 (1989).

[20] M. D. Amatangelo, D. E. Bassi, A. Klein-Szanto, and E. Cukierman, Am. J. Pathol. **167**, 475 (2005).

[21] C. Jones, M. Cibula, J. Feng, E. Krnacik, D. McIntyre, H. Levine, and B. Sun, Proc. Natl. Acad. Sci. U.S.A. **112**, E5117 (2015).

[22] S. van Helvert and P. Friedl, ACS Appl. Mater. Interfaces **8**, 21946 (2016).

[23] S. Nam, K. Hu, M. Butte, and O. Chaudhuri, Proc. Natl. Acad. Sci. U.S.A. **113**, 5492 (2016).